Design and manufacturing of a novel continuous casting technique for the addition of ceramic particulate reinforcement, alloying elements and grain refiners in Al-system

[a]Prasenjit Biswas, [a]Amrik Kundu, [b] Hiren R. Kotadia, [c]Archana Mallik, [a]Sanjeev Das*
[a]Advanced Metal Casting Laboratory, Department of Metallurgical and Materials Engineering, National Institute of Technology Raipur, G.E Road, Raipur - 492010, India
[b] Warwick Manufacturing Group, The University of Warwick, Coventry, UK
[c]Department of Metallurgical and Materials Engineering, National Institute of Technology Rourkela, Odisha – 769008, India
Email: sanjeevdas80@gmail.com

Abstract

Processing of aluminium and its alloy in an economical way is still a big challenge for the industry. In the present work, a novel continuous casting set-up has been designed and manufactured to introduce alloying elements, particulate reinforcement and grain refiners in any Al system by implementing mechanical force convection and bottom-feeding of elements or particles in liquid aluminium. The main objectives behind the design are to minimize capital cost, running cost, time, energy consumption and defects in the cast products. The present set-up does not lead to vortex formation during mixing to disperse the particles. Thus, there is less possibility of entrapment of gasses and hence subsequent formation of casting defects is comparatively fewer. A detailed study on the various temperature zones in the set-up has been accomplished using a data logger. The cast alloy, metal matrix composite and grain refiner added aluminium alloy were subjected to optical microscopy, scanning electron microscopy and X-ray diffraction studies. The results showed uniform distribution of reinforcement particles and alloying elements in metal matrix composite and commercial pure aluminium alloy, respectively. Grain refinement in aluminium alloy was also observed after the addition of grain refiner. A cost analysis study of the casted product showed that, the present proposed process is comparatively economical than the conventional available process.

Keywords: Continuous Casting Process; Mechanical force convection; Bottom feeding; Al Metal Matrix Composites; Al Alloy; Grain refiner addition

1. Introduction

Aluminium (Al) is undoubtedly, one of the most focused materials in automotive, aerospace and construction industries as it is replacing steel and other material due to its low temperature processing, high specific strength, corrosion resistance, and excellent formability [1,2]. However, to get better comparative properties as a replaced material, the modification in the microstructure with enhanced strength through alloying, composite fabrication and grain refinement of alloys are in practice in Al system [3–6]. Alloying is a conventional alternative to enhance the inherent characteristic properties of Al. Many researchers have substantiated that adding various types of alloying elements, significantly contribute in enhancing the microstructural and mechanical properties of the developed Al alloys [7]. Reinforcing Al with particles/whiskers/fibres of ceramics/metals to make Al metal matrix composites (Al-MMCs) has emerged as a promising engineering material with increased strength, stiffness and wear resistance. However, achieving a homogeneous distribution of the reinforcement is a major challenge during the production process [8]. The addition of grain refiner (GR) is one of the well-established approaches in which the GRs act as a heterogeneous nucleation site to refine the structure[9]. However, for all the mentioned modifications, homogeneous mixing of the added elements is an essential condition. Hence, processing techniques have become important to meet all the required parameters. The optimization of the process from the economical point of view is of significant interest to many researchers [8,10]. Various production techniques and their challenges to manufacture the above Al base materials are discussed below.

Adding non-wetting solid particles to molten Al alloy has often been attempted to modify the strength, hardness or other mechanical and structural characteristics of the Al alloy [11]. However, it is challenging to add non-wetting particles in liquid Al. The addition of elements like, magnesium (Mg) can also increase the wetting of the particle, which assures dispersion of non-wetting particles [12]. The homogeneous mixture of particles in the melt can be achieved by using mechanical stirring [13]. Even so, the process is not completely flawless for large volumes of casting especially for industrial-scale production. Al-MMCs can also be produced by powder metallurgical route, which is relatively expensive, limited to smaller dimension products and batch type process with a low success rate [14]. The liquid metallurgical process like stir casting and infiltration is the most practiced process for particulate reinforced Al-MMC production. Hence, stir casting process has been implemented by some researchers, with optimization of impeller type and angle, rotation per minute (rpm), baffle placing, particle size, and other processing parameters to enhance the mixing [8,15].

Junwen Zhu et al. also implemented stir casting with a squeeze casting system to prepare Al-SiC reinforced MMC [16]. The process includes the molten composite mixture prepared in a stir casting system which was incorporated in the squeeze casting system under standard operating conditions. The results show a uniformly distributed reinforcement in the MMC with improved mechanical properties can be achieved with this system. However, it has been observed that most of the prior practiced processes are expensive with inhomogeneous dispersion of particles, complex processing, and batch type production route. Hence, the production of particulate Al-MMC is not a successful practice in the recent industrial scenario.

In general practice, Al alloys are produced by powder and liquid metallurgical route. However, many techniques have been developed in the process of Al alloy making, which illustrate that to disperse the alloying element, elements are added in large furnaces in Al melt followed by holding and mixing process [17]. Hence, controlling of production rate significantly depends on the size of the furnace. For a large amount of alloy production batch type furnace are time-consuming and, for small scale production, large furnace operation is significantly expensive. Also, the homogeneous distribution of the alloying element throughout the casted product still is a major lacuna for the industry and researchers are working to optimize conventional batch type melting and casting process. Apart from the above conventional techniques, few researchers have also focused on various new techniques to prepare Al-alloys e.g. Jiang et al prepared Al/steel bimetal with compound casting [18]. Jiang et al. also used compound casting method to produce Mg/Al bimetal by implementing a few modifications in the casting process [19].

The strength and plasticity of Al alloys are dependent on grain size to a great extent, thus improvements in these properties can be achieved by controlling the grain size through the addition of GRs viz. TiBAl, AlTiC, etc. [9]. Nevertheless, a few more other techniques involved in grain refinements are ultrasonic treatment, electromagnetic agitation, mechanical stirring during solidification, rapid solidification and severe plastic deformation [9,13]. Grain refinement by adding GRs are usually employed in the industry due to its simplicity and flexibility, of the process involved. However, several issues of agglomeration, homogeneous distribution, or settling of the refiner and porosity hamper the efficiency of the process [20]. In general, industrial practice, GR rods are directly dipped inside the Al melt for dispersion without stirring. However, the process is not very efficient to disperse the GR efficiently for grain refinement.

Implemented liquid metallurgical routes like stir casting process to make composite and alloys are batch type, expensive, and time-consuming process even after having several casting defects and difficulties. However, getting uniform distribution of particles and the alloying element is also a big challenge for the industry. Hence, in this present work, a novel continuous casting set-up has been introduced to overcome the present challenges by integrating the mechanical force convection technique along with bottom-feeding technology. The developed setup is different from other existing conventional Al casting methodologies and technology in terms of its design and working principle. An attempt has been made to assess the efficiency of the process to produce continuous particulate Al-MMCs and Al alloys, which, also has a unique attachment that can introduce GR into the molten Al by achieving a homogeneous fine grain structure. Additionally, experimental investigation and cost analysis of the developed casted ingot have been carried out for further validation of the setup as well as its casting capabilities in terms of quantity, run time, casting defects, optimum cost-efficacy, etc.

2. Experimental Methodology

The primary focus of the present research is to design an economical casting technology to produce versatile Al-based materials including casting of different alloys and composites and addition of GRs. In the conventional process, vortex formation is essential to incorporate the particles or elements into the liquid metal. However, in this process, vortex formation is completely eliminated. The complete process is continuous as the continuity in the melt flow in the set-up is maintained. Accordingly, this segment will describe the experimental methodology and its validation in detail followed by the characterization part. Flow chart 1 shows the complete steps involved in the process.

2.1. Casting technology: Process and design

Fig. 1 shows the experimental set-up which includes the 3D schematic line diagram generated by using Sketch-up and AutoCAD software, real lab-scale set-up developed based on the design and a casted ingot using the set-up. The design is a set-up to continuously cast Al alloy/composite ingots. Different parts of the set-up can be followed from the figure (Fig. 1a) and the entire design has four significant segments i.e. pouring channel, mixing chamber, high shear device, and the output channel. The pouring channel includes a pouring basin (1), flow channels (2, 3, and 4). Channels 2 and 4 are for molten metal flow, whereas channel 3 is for the addition of element/master alloy or reinforcement particle or GR. In the present

investigation, Al was melted in a pit furnace (outside of the set-up, up to 900º C to maintain the superheat) and carried to the pouring basin by a crucible. As the metal reaches to channel 4, addition of master alloy/ reinforcement/ grain refiner (MRG) was commenced through channel 3 for dispersing it with the base metal. For mixing of the molten metal through mechanical convection, a high shear device (9) is the next significant component of the design set-up, which is a bottom-feeding technique of added advantages. Hence, the molten metal along with MRG entering the mixing chamber, has to go through 9. Mentioned numerals 11-16 are the various parts of 9 which have been elaborated below and are presented in Fig. 1(a). The device has an arrangement of a 40 mm height four-headed blade (16) attached to a shaft (15), which ensures adequate mixing as well as contact of the liquid and MRG. 15 and 16 are housed in a stator (13) and the distance between the stator wall (13) and blade (16) has been maintained as low as possible (1.5 mm in the present case) so that the particles cannot skip the contact of blade. 13 has a perforated bottom (containing ø2 mm holes) leveled as splash part (12), which assists flow of the mixed liquid hot metal towards the mixing chamber through a pressure difference mechanism. The distinctive design of 9 ensures that the MRG will breakdown by high shearing force imposed by 16 and mix with the liquid metal and flow towards the mixing station (7).

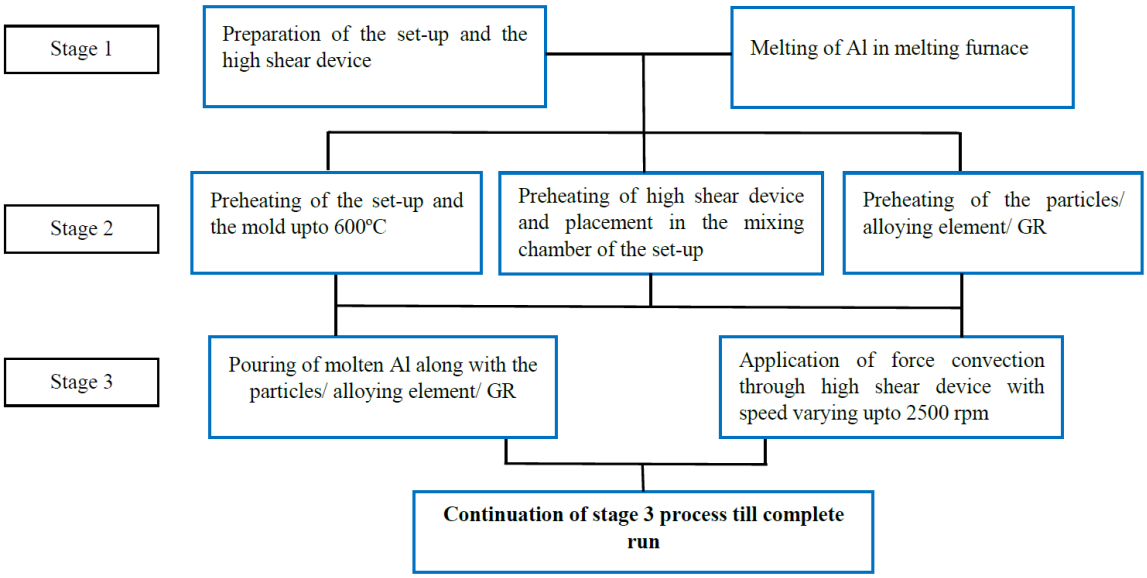

Flow Chart 1: Details of continuous cast process

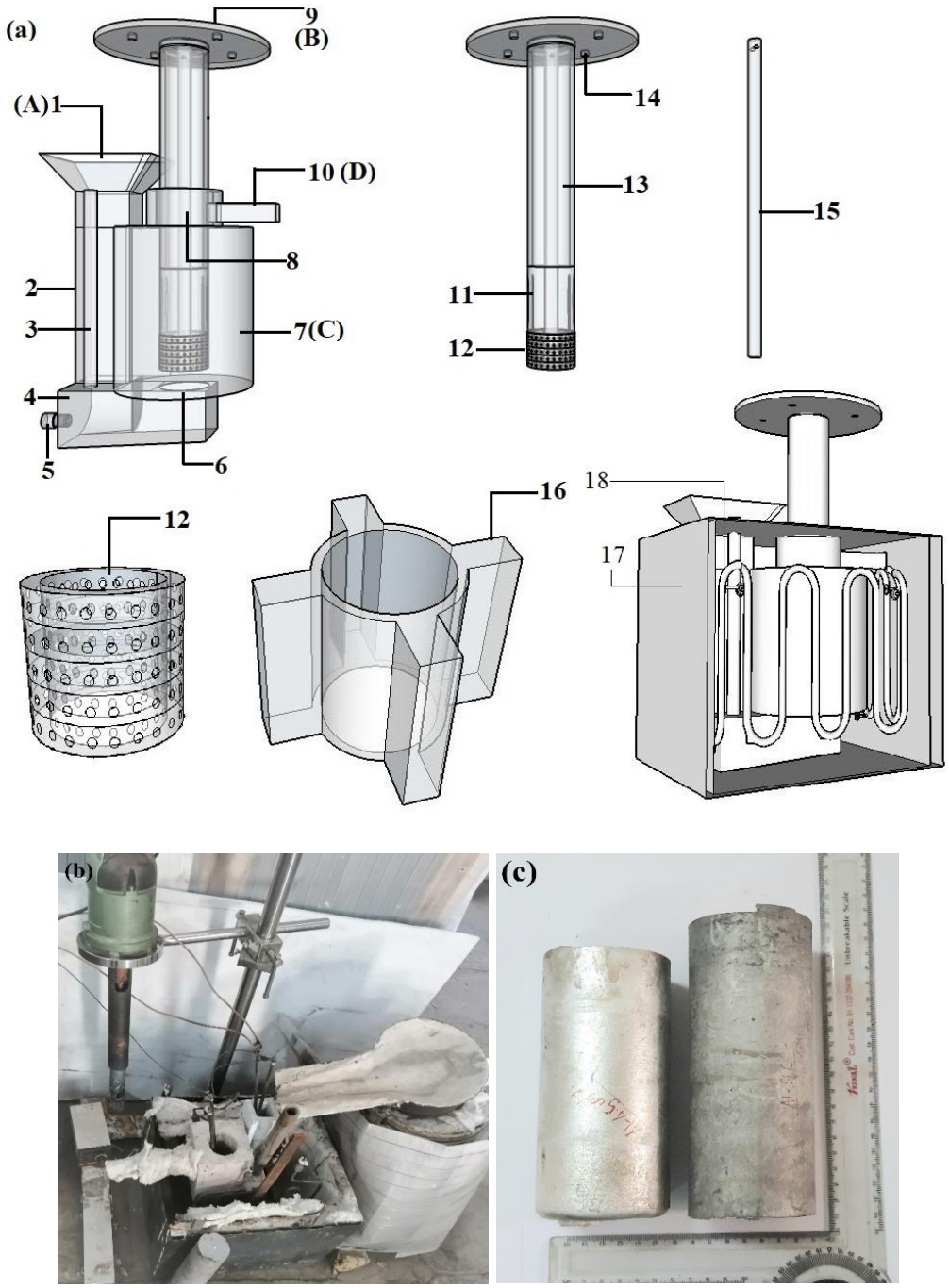

Fig.1: Experimental set-up of continuous casting process (a) 3-D schematic of the design (b) prepared lab scale set-up (c) casted ingot

Numerals used in Figure 1(a)

1. Pouring basin
2. Vertical pouring channel
3. Channel to add an alloying element, reinforcement and grain refiner/modifier
4. Horizontal pouring channel
5. Valve
6. Buffer
7. Main mixing chamber
8. Small cylindrical chamber
9. High shear device
10. Output channel
11. An oval shaped (preferable) section for cleaning
12. Splash part
13. Rotor-stator chamber
14. Holding plate of the motor
15. Shaft
16. Four headed blade
17. Ceramic fibre board
18. Heating arrangement

The said claim can be followed through the tailing analysis: as the flow in 1 continues, pressure in the mixing chamber builds up, and mixed metal rises in 13 up to level of 12. The high pressure would try to push the hot metal to splash vigorously, however, the small opening in the splash does not allow to do so. Rather it disintegrates the MRG if required and results in forceful exit of the hot metal, leading to uniform mixing of the mixed metal liquid. Further 9 has an elliptical shape cut (11) just above 12, which is advantageous in two ways: (i) it would enable to clean off the sticky metal of the high shear device and (ii) control the flow of mixed molten metal in 9. If the metal mixture gets jammed in 12 then it may go up into the motor creating undue issues. Therefore, the process prohibits the overflow of the mixed molten metal and allows it to easily come out from 11 to the mixing station. Finally, the shearing device is set at a required speed by an attached motor through the holding plate (14) from the top. Then after the operation starts in the mixing channel, which essentially consists of a buffer (6) and the main mixing station (7). Molten Al along with MRG flows through 4 and 6 to 7. In this report, 9 was pre-heated (up to 600ºC) and was placed just at the top of 6. The shaft was rotated at 2500 rpm, which creates mechanical force convection inside 9. For the maintenance and the cleaning purpose of the channel, a valve (5) has been created whose size can be varied as per the requirement and flexibility of the practical set-up. The main emphasis of the valve (5) is to clean the metal which will stay in the chamber after the complete continuous run of the metal. Further a small cylinder (8) is attached at top of mixing station to connect the mixing chamber to output channel. The purpose of the small cylinder is to minimize the loss of metal volume in the device after mixing. Finally, the melt is tapped and casted into billets through output channel (8). The entire set-up was pre-heated up-to 600 ºC with the heating arrangement (18) to minimize the temperature loss and to maintain the fluidity of the molten metal inside the respective chambers.

The materials used for the design are alumina ceramic for mixing station and N17 ceramic insulation board by using ceramic TC as an adhesive (to make leakage proof setting). To insulate the set-up and reduce heat loss, set-up was covered and packed with the N17 ceramic board (17).

2.2. Casting technology: Process validation

To validate and testify the proposed design for proper casting, attempts have been made to produce an Al-based binary alloy, MMC with an Al alloy matrix and ceramic reinforcement and refined grain castings. The binary Al alloy chosen for the current study was Al with 4.5

wt.% Cu. Commercially pure Al (99.9%) was used to make the alloy whose temperature was maintained at 900 ºC in the caster to keep it liquid enough for addition of alloying elements. For maintaining the stoichiometric composition of the alloy, a master alloy with 40 wt.% Cu was prepared and then a calculated amount of the master alloy was added to the caster to achieve the required composition of 4.5 wt.% Cu and rest Al. The master alloy was pre-heated up-to 400 ºC before adding it into the caster. Al-6082 alloy used in the present study is to synthesize the MMC. The reason for selecting the particular alloy is its moderate strength and excellent corrosion resistance. Silicon carbide (SiC) particles have been used in this study as a reinforcement particle to make the MMC composite. The reinforcement was added in the form of green pellets of ø 20 mm. Before charging the reinforcement, mould and SiC pellets were preheated up to 400 ºC to remove any inherent moisture and develop a surface treatment to increase the wettability of SiC particles in liquid Al alloys [21].

Table 1: Compositional description of Al-6082, GR and details of reinforcement

Elements of Al 6082 Alloy								**Reinforcement particle**	**Grain refiner**
Si	*Mg*	*Mn*	*Fe*	*Cr*	*Cu*	*Zn*	*Al*	*SiC particle Size in μm(5 wt.%)*	*Al-5Ti-1B (wt%)*
1.2	0.78	0.50	0.33	0.14	0.08	0.05	Balance	2-10	2

Commercially available Al-5Ti-1B master alloy was added in the liquid Al 6082 alloy (2 wt.% of alloy) to study the effect of grain refinement. The addition of the GR followed the same routine as that of alloy casting mentioned above. Mixing of GR was performed by using the mechanical force convection technique. After solidification, the sample was taken out from the casted ingot to observe the grain size and the effect of the GR. Table 1 shows the composition of the mentioned alloy and GR and details of SiC.

2.3. Characterization of the castings:

Depending upon the type of casting, various characterization techniques have been adopted including porosity, density measurements, structure and phase analysis by microscopy and XRD techniques. The adopted methodology/techniques have been elaborated as follows:

Experimental density has been calculated by using the Archimedes principle for Al 6082-2wt% SiC, Al-4.5wt% Cu and Al 6082 with 2 wt.% Al5Ti1B alloy. The experimental density ρ_{ex} of composites was calculated following equation 1 [22]:

$$\rho_{ex} = \frac{P}{A}\rho_0 \ldots\ldots\ldots\ldots\ldots\ldots\ldots\ldots\ldots (1)$$

Where ρ_{ex} is experimental density, P is weight in the air, A is weight in water and ρ_0 is the density of the liquid medium at elevated temperature. Rule of mixture has been used to calculate the theoretical density ρ_{th} of Al-4.5Cu binary alloy as given in equation 2 [20],

$$\sum \frac{c_i M_i}{c_i V_i} \ldots\ldots\ldots\ldots\ldots\ldots\ldots\ldots\ldots (2)$$

Where c_i is the concentration of the material, M_i is the molar mass, V_i is the molar volume of the element. Similarly, the rule of the mixture was used to calculate the density of the composite and the grain refined alloy. Equation of rule of mixture to calculate the theoretical density of composite and grain refined alloy is given in equation 3 [22],

$$\rho_{th} = \rho_1 c_1 + \rho_2 c_2 \ldots\ldots\ldots\ldots\ldots\ldots\ldots\ldots\ldots (3)$$

Where, ρ_1 and ρ_2 is the density of the added compound and $c_1$and c_2 are the concentration of the same. The volume of the porosity, which means its size and distribution in the fabricated Al-MMC's plays a crucial role in affecting the mechanical properties. The porosity of the fabricated composites can be determined following equation 4 [22],

$$\text{Porosity } (\%) = \frac{\rho_{th} - \rho_{ex}}{\rho_{th}} \ldots\ldots\ldots\ldots\ldots\ldots\ldots\ldots\ldots (4)$$

Light optical microscope (OM, Leica S8 APO), as well as scanning electron microscope (SEM, Zeiss EVO 18), were employed to characterize the microstructure of polished samples of the binary Al-Cu alloy, composite, and grain refined alloy. Specimens were prepared following the routine procedure of metallographic sample preparation and they were examined under SEM to check the particle size and distribution of the reinforcement in the alloy matrix. Comparison of the grain size was done by analyzing both the grain refined and non-refined Al 6082 alloy. The grain size of the grain refined Al-6082 alloy has been measured utilizing image analyzer software (ImageJ). However, to check the homogenization of the grains, macrostructures have also has been observed. X-ray diffractometer (XRD, Pan Analytical X'Pert) with Cu (K_α) radiation has been employed to identify the phases formed in Al-Cu alloy, reinforcement phase in composite and to check the trace of grain refinement in the alloy with a scan range of 20º-120º and a scan rate of 0.026º/sec.

3. Results and discussion

The results and discussion section comprises of temperature profile of various zones of the novel continuous casting set-up during the casting process, porosity and density measurement, and optical and electron microstructural characterization of the cast billets.

Temperature of the melt is directly related to important factors, which determines the quality of the cast billets, i.e., flowability, wettability, distribution of the second phase, and solidification of the Al-based product. The temperature variation across different zones was read by thermocouples placed and dipped in the marked zones of Fig. 1(a) (A, B, C, D). Then the temperature data with time of casting was recorded and analysed by the data logger (Keysight Data Acquisition System, DAQ970A). Fig. 2 shows the temperature profile of different zones in the set-up i.e. pouring channel, high shear device, mixing chamber, and output channel.

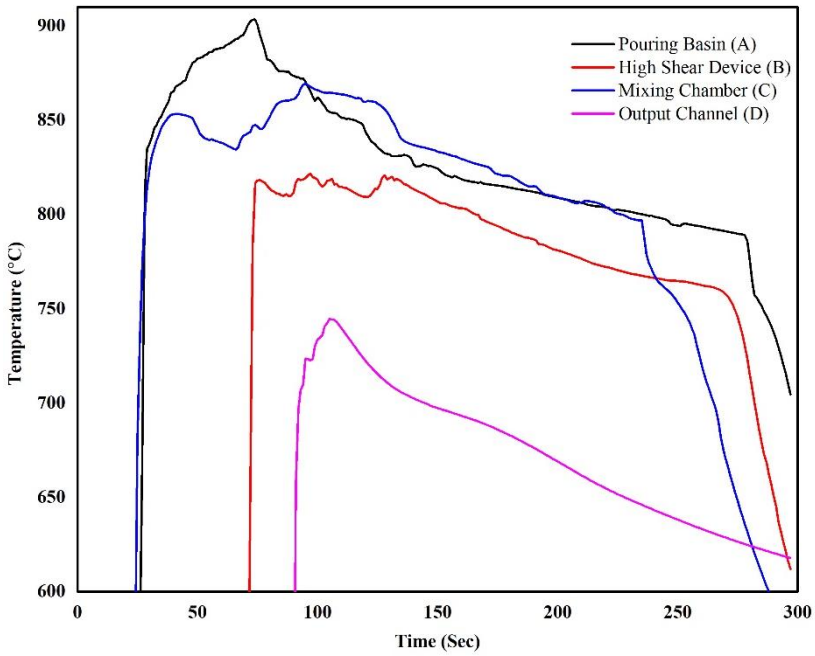

Fig.2: Temperature profile for Pouring channel (A), High shear device (B), Mixing chamber (C), Output channel (D)

The aforementioned analysis was done only for Al-6082 alloy casting as there was no significant difference of profile in the continuous flow system during any of the casting systems. All the profiles have basically three zones, an increasing temperature zone, an almost plateau zone, and then a decreasing region. Each region signifies variations during the process, which will ultimately decide the quality of the cast. The falling temperature zone has less importance as it is the period at which the experiment is about to complete, and one should look for a uniform and extended constant temperature region till 250 seconds. Fig. 2 (A) shows the time-temperature data for the pouring basin (1). As the pouring started, temperature in thermocouple instantly reached to 830 ºC. Thereafter, a gradual rise and fluctuation are observed from 830 ºC to the poured melt temperature of 900 ºC within around 75 s due to the

heat exchange between the molten metal and the surface of the pouring channel. Then temperature falls off and remains almost constant for 280 seconds and then finally decreases continuously. Fig. 2 (B) illustrates the time-temperature plot of the high shear device (9) used for mechanical force convection and homogenization of liquid metal. Initially, the preheated high shear device (9) was attached in the system before the start of the process, due to which the plot shows a similar increasing trend as the pouring channel. As the metal comes in contact with the high shear device (9), the rotor was turned on. The temperature profile in the set zone showed a high fluctuation at a temperature of 825 ºC for around 60 seconds, which was due to the homogenization of the molten metal temperature with the effect of forced convection. The liquid metal gradually came in contact with the high shear device (9) and started absorbing and releasing heat to attain an equilibrium temperature point. Thereafter, as the pouring melt temperature decreased, the temperature in the high shear device also decreased accordingly. Temperature losses are quite significant from the pouring basin to the high shear device, which could be due to the heat transfer from the molten metal to the high shear device (9). Fig. 2(C) shows the time-temperature data for the mixing chamber (7). Temperature variation in the high shear device (9) also affects the temperature of the stored liquid metal in the mixing chamber. After 100 seconds, the temperature started to decrease slowly, which was due to the completion of the homogenization process, and the temperature loss with time. The temperature of the mixing chamber (7) is slightly higher from the high shear device (9) as the high shear device (9) was preheated to a relatively lower temperature (450 ºC) than the mixed chamber (600 ºC). Also, the volume of metal in the mixing chamber is higher as compared to the shear device. However, the study implies that the temperature loss inside the set-up, i.e. the mixing chamber (7) and the high shear device (9) is very minimum. Fig. 2(D) shows the time-temperature plot for the output channel of the set-up. As the set-up is designed for the lab-scale casting of 10 min duration, the drop of temperature is observed as the pouring stopped. However, for prolonged industrial-scale casting, a uniform temperature can be achieved after a certain period. Initial temperature loss was observed during pouring, where, the metal came in contact with the air. The output channel delivers the homogenized metal which has a comparable temperature as the mixing chamber (7). The continuous flow in the system also ensured equilibrium in temperature accordingly with minimum temperature losses.

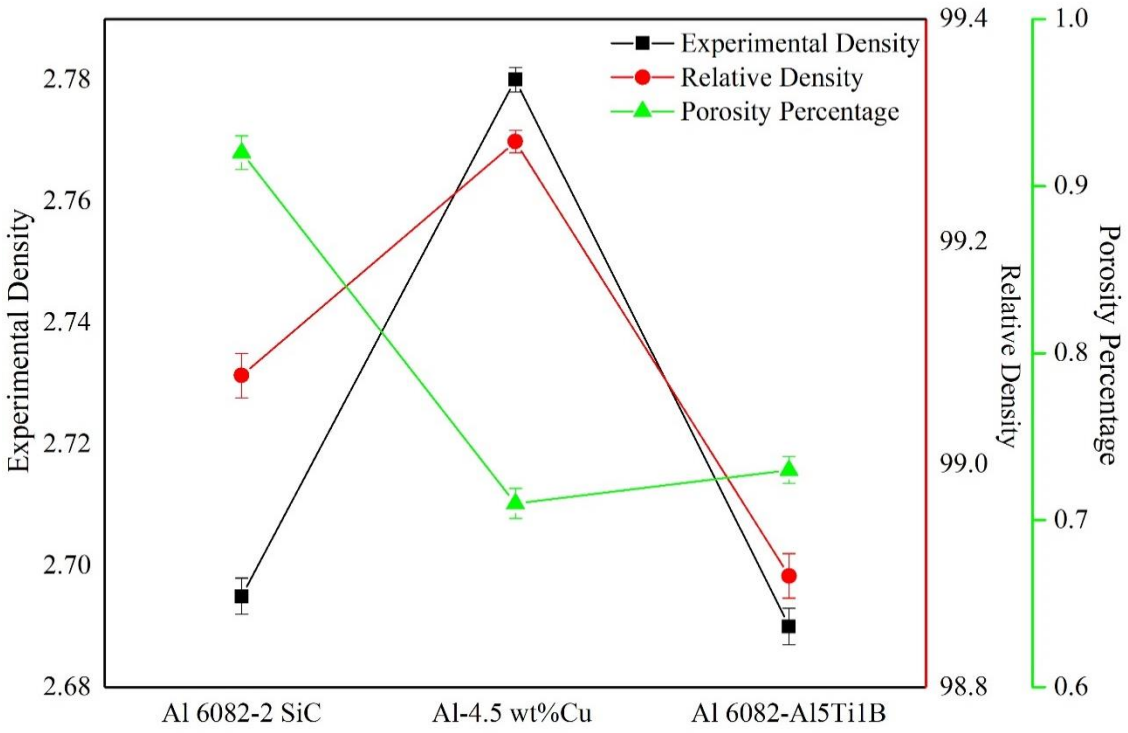

Fig. 3: Porosity percentage vs. relative density vs. experimental density of cast Al-MMC, Al alloy and grain refined Al 6082 alloy

The efficiency of the set-up can be validated by the quality of the product starting with its density and indigenous porosity. Kandpal et al. described that porosity generally occurs due to the entrapment of gas, hydrogen entrapment due to de-gasser treatment, foreign particles or inclusion, improper mould preparation [23]. Porosity percentage and relative density have been measured by the procedure said in the methodology part. Fig. 3 shows the porosity percentage along with the experimental and relative density. For relative density, Al-4.5 wt. % Cu shows better results in comparison to the composite and grain refined alloy. As the alloy contains an intermetallic in the system and was formed due to a chemical reaction, its density might have been more than the base Al. The addition of reinforcement makes the matrix lighter, due to which composite material generally turn into lighter than the parent matrix alloy. In the case of grain refinement, casted ingot showed a high porosity percentage and lesser value of density as compared to the base alloy. It can be attributed to the remelting of the alloy and Al_3Ti phase formation during solidification [9]. For Al6082 with Al5Ti1B GR rod as well as for Al-4.5wt% binary alloy, the percentage porosity shows less than 1%. Similarly, for the composite, the porosity percentage is around 1%. Commercially produced stir casted Al-SiC MMC shows a porosity percentage ranges from 0.09- 12.45 %[24]. Hence, it will not be overstated to state at this juncture that the casting quality is significantly good. Generally, porosity occurs due to

entrapment of gases and vortex formation during the casting process. Vortex formation has been eliminated in this methodology due to bottom feeding. Furthermore, the bottom-feeding of liquid metal along with element or particle or GR towards the mixing station avoids the incorporation of gases from the environment as the complete set-up is covered and insulated.

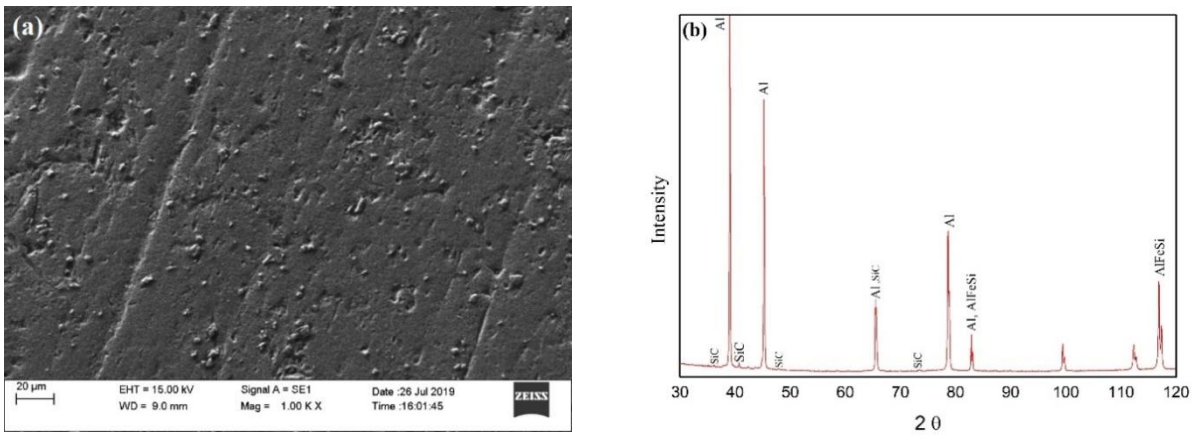

Fig. 4: (a) SEM microstructure (b) XRD plot of as cast Al6082-2 wt.% SiC MMC

After a thorough analysis of density and porosity, an attempt has been made to analyse the distribution of reinforcement in Al-MMC, formation of alloy and evidence of grain refinement through microscopic and phase analysis. Fig. 4 (a) shows a lower magnification SEM microstructure of the Al6082-2wt% SiC MMC collected from the ingot. The white particles are the SiC particles, which shows it's homogeneous distribution throughout the matrix. Elemental analysis of the matrix and SiC particles are presented in supporting documents (Fig. S1). XRD analysis of the composite was also carried out and has been shown in Fig. 4(b). Signals from both the matrix and reinforced particles can be observed in the diffractogram, hence confirming the distribution. Along with the phases, presence of AlFeSi can be seen from Fig.4 (b), which might be due to impurities present in the raw materials. Distribution of the reinforcement particle over the matrix is one of the key influencing properties for the composite material. The composite samples were investigated to check the particle size and the inter-particle distance with image analyzer software (ImageJ). Measured average particle size and the inter-particle distances are 3.5±0.25 µm and 12.6±5 µm, respectively.

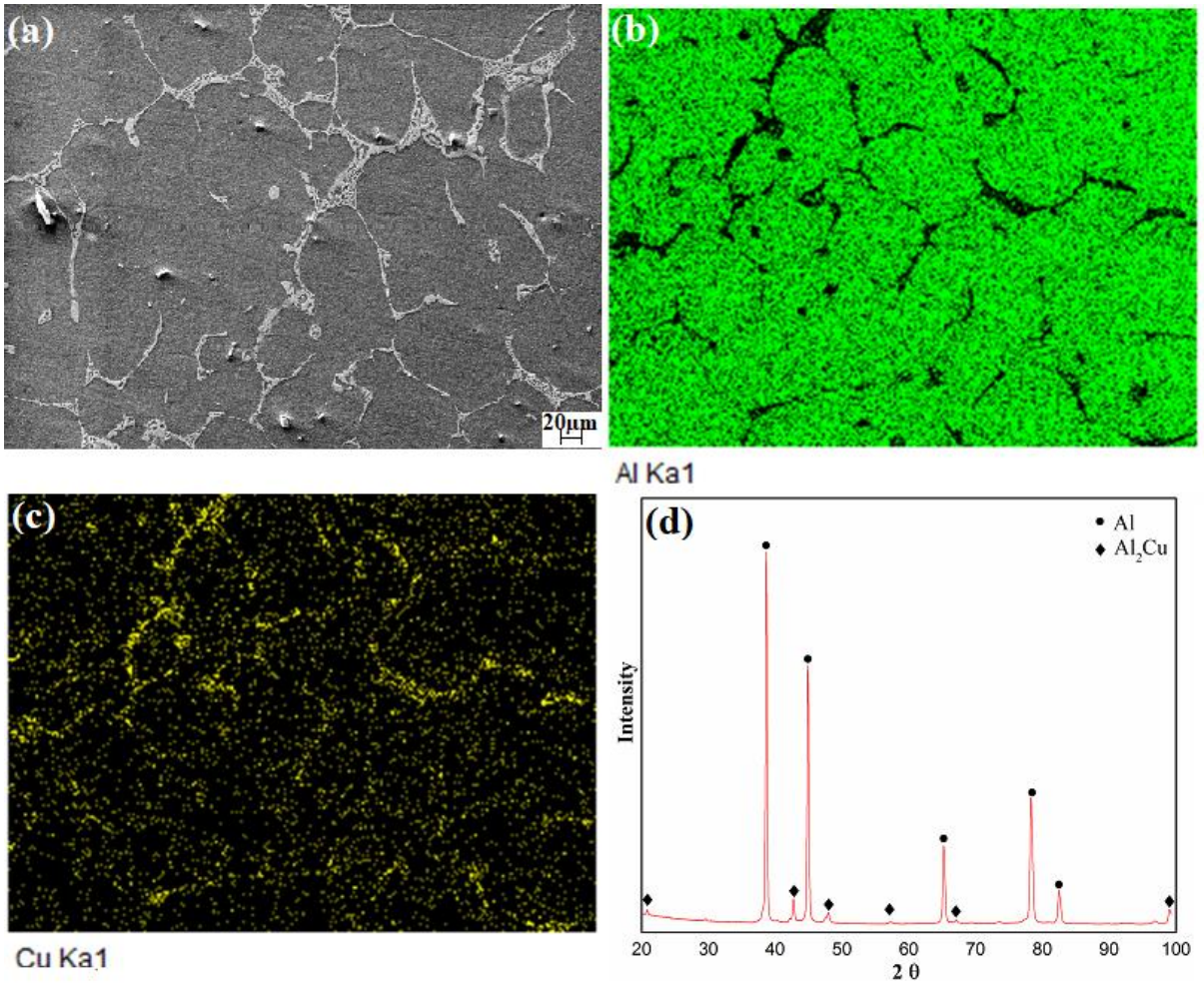

Fig.5: (a) SEM microstructure, Elemental mapping (b) Al (c) Cu and (d) XRD plot of Al-4.5Cu alloy

Fig. 5 a, b, c and d shows the SEM micrograph, elemental distribution of Al and Cu and XRD plot of Al-4.5 wt.% Cu binary alloy. In the said methodology, the master alloy has been used to make Al-4.5 wt.% Cu binary alloy through a continuous casting process with a mechanically forced convection method. There is no extra holding time during the mixing and processing of the alloy. To observe the formation of intermetallic phases in the microstructure, XRD analysis has been carried out. Bright inter grain-like structures throughout the micrograph can be observed from Fig. 5 a. It is believed that these are segregation of Al_2Cu intermetallic phase at the grain boundaries, which has been confirmed by elemental analysis as presented in supporting file (Fig. S2). Moreover, the uniform distribution of Al and Cu can be observed from Fig. 5 (b) and (c). XRD (Fig. 5 d) analysis of the alloy shows high-intensity peaks of Al as well as of Al_2Cu phase, which further confirms the formation of alloying. By controlling the master alloy feeding rate, alloy composition can be varied from the present experimental set-up.

To get a homogeneous fine-grained structure throughout the material, mixing of GR is very significant. Fig. 6 (a-d) shows the structure of Al 6082 alloy without and with GR, at low and high magnifications. Confirmation of presence of GR is done through individual elemental analysis and can be followed from Fig. S3 and S4 (supporting documents). The structure as shown in fig. 6 (b) depicts homogeneous macrograph of fine grain structure, whereas the alloy without added GR (fig. 6 a) shows the coarser rosette shape structure.

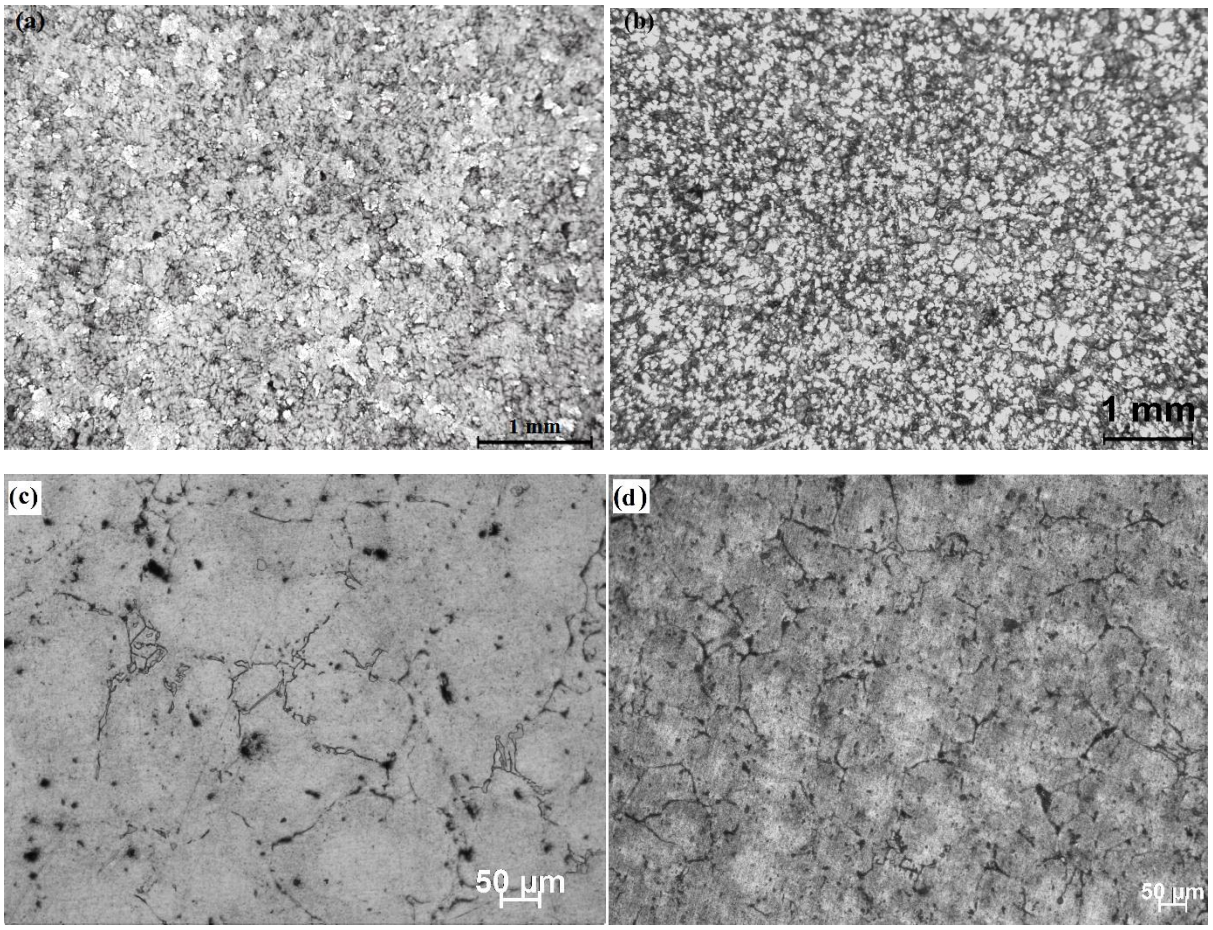

Fig.6: Macrostructure (a) without grain refiner (b) with refiner, Optical Microstructure (c) without refiner (d) with refiner of Al 6082 alloy

The effect can be followed more clearly at higher magnification as shown in fig. 6 c and d. The grain size of the refined and non-refined structure has been measured. The average grain size of the refined structure is 93±11µm and non-refined structure is 194±16 µm which confirms that addition of 2 wt.% of Al5Ti1B GR exhibited around 52 % reduction in the grain size. Hence, the results do validate that the proposed methodology is suitable for grain refinement while casting Al ingots.

4. Cost Analysis

For the success of any production technology, apart from the quality of its product, flexibility, simplicity, the volume of production, the economy of production process plays a vital role to commercialize any technology. Hence, this section has the most significant contribution towards the adaptability, acceptability and saleability of the proposed technology and needs special attention before conclusion of the investigation.

Researchers have proposed various methodologies to find out the cost of casting, among which the most evidential techniques are based on intuitive, analogical [25,26], analytical [27], feature-based [28,29] and parametric [30,31] studies. Other methods in practice are to find out the component cost by weight of output, scrap, time of production, etc. For large amounts of production, these methodologies can be used with a percentage of error. However, the major cost elements of casting are material, tooling, labor, energy, and overheads which were identified by early researchers. In the present study, to do the approximate estimation of the casting cost incurred in each case, a mathematical model explained by Chougule et al. has been used which is linked to a web-based intelligent collaborative engineering system called WebICE [32]. Cost of casting for the given lab-scale experimental set-up can be computed through equation 5:

$$C_{casting} = C_{material} + C_{labour} + C_{energy} + C_{tooling} + C_{overheads} \dots\dots\dots\dots\dots\dots\dots (5)$$

Where $C_{casting}$ = Total cost of the casting, $C_{material}$ = Cost of the material, C_{labour} = Cost of labor, C_{energy} = Cost of energy, $C_{tooling}$ = Cost of tooling, $C_{overheads}$ = Cost of overheads. The present work mainly focusses on the total cost of casting with respect to the cost of materials. Other costs have not been considered in the current scenario for the estimation of cost. Incorporating other miscellaneous costs, the total cost of the casting comprising labor, energy, tooling, and overheads can also be calculated.

Cost of material can be further classified through equation 6 as,

$$C_{material} = C_{direct} + C_{indirect} \dots\dots\dots\dots\dots\dots (6)$$

Where, C_{direct} = Direct Cost, $C_{indirect}$ = Indirect Cost whose calculations are presented below:

$$C_{direct} = [(C_{metal} * w_{metal}) + (C_{element} * w_{element})] * f_{melting} * f_{pouring} * f_{fettling} \dots\dots\dots (7)$$

Where, C_{metal}= Cost of Metal, w_{metal} = Weight of Metal, $C_{element}$ = Cost of Element, $w_{element}$ = Weight of Element, $f_{melting}$ = Factor for metal loss in melting, $f_{pouring}$= Factor for metal loss in the pouring, $f_{fettling}$ = Factor for metal loss in fettling.

According to Chougule et al., the values for the above mentioned three factors have been taken as 1.01 considering the minimum metal loss in the casting set-up [32]. The weight of the metal and the weight of the element for a given casting can be calculated through, $w_{metal} = w * w_{f_{metal}}$ and $w_{element} = w * w_{f_{element}}$. Where w = Weight of cast, $w_{f_{metal}}$= Weight Fraction of metal, $w_{f_{element}}$ = Weight Fraction of element. Indirect cost is calculated through equation 8:

$$C_{indirect} = \text{cost of high temperature adhesive for casting set up } + \text{cost of accessories} \ldots \ldots \ldots (8)$$

In the present work, the total cost has been calculated taking into consideration of direct and indirect costs and is presented in Table 2. The basis of calculation, i.e. $w = 10\ kg$ has been considered. Indirect cost remains same for all the casted structures as it has only cost of high temperature adhesive for casting set-up ($ 9.43 per 10 kg of casting) and cost of accessories ($ 6.08 per 10 kg of casting). Hence, the indirect cost comes around $ 15.51 per 10 kg of casting as shown in equation 10.

$$C_{indirect} = \$\ 9.43 + \$\ 6.08 = \$\ 15.51 \text{ per 10 kg of casting}$$

Table 2: Cost analysis of Al-MMC, GR-alloy and Al-alloy for 10 kg of casting

Al casting type	Weight of Commodities (kg)		Cost of Commodities ($)		Direct Cost per 10 kg of casting (C_{direct}) ($)	Indirect Cost per 10 kg of casting ($C_{indirect}$) ($)	Cost of material per 10 kg of Casting ($C_{material}$) ($)
	Weight of metal (w_{metal})	Weight of element ($w_{element}$)	Cost of metal per kg (C_{metal})	Cost of element per kg ($C_{element}$)			
MMC (Al–2 wt.% SiC)	9.80	0.20	5.66	11.31	59.48	15.51	74.99
GR (Al-2 wt.% Al5Ti1B)	9.80	0.20	5.66	11.60	59.54		75.05
Alloy (Al-4.5 wt.% Cu)	9.55	0.45	3.11	5.94	33.35		48.86

In the present case, the values of $f_{melting}, f_{pouring}\ and\ f_{fettling}$ is taken as 1.01, however, in the case of conventional casting values would be greater than 1.01. Therefore, the direct cost

and subsequently, the cost of the material for conventional casting would be greater than the direct cost and cost of the material involved in continuous casting.

Cost reduction is highly influenced by batch type or mass type production. As the present methodology illustrates a continuous casting technique, the cost of the product is automatically reduced from conventional techniques. Other constituent factors like the rejection factor are comparatively less or can be neglected in the process. As the set-up has no such complication to have the losses in the melt, so the metal loss values are reduced to a minimum. By considering all the key factors, it can be summarized that the cost of the present technique is much lower than the other conventional techniques. Few factors like accessories and maintenance are fixed for a specific casting set-up, so they will remain the same independent of the volume of the casting. So, to get an optimum level of production and minimized casting cost, a continuous casting method seems to be highly beneficial. Hence, cost varies indirectly proportional to the volume of production. Mathematically, the cost of casting follows a direct relationship with a fixed cost and is inversely related to the volume of casting i.e. as the production quantity increases the total costs involved decrease considerably.

5. Conclusion

Present investigation is an attempt to design an economical casting process to cast Al base ingots through continuous casting. The proposed process has been validated by casting Al matrix composites, Al alloy and grain refinement of a commercial Al alloy. The cost-effectiveness of the process has been evaluated through a thorough analysis of the expenses incurred during the casting process. Following are the salient concluding remarks of the research:

- The setup is a unique design to continuously cast Al alloy, Al MMCs and GR Al alloy. It consists of a novel technique, which combines bottom-feeding and mechanical force convection to incorporate master alloy/reinforcement/grain refiner in Al system. The design has eliminated vortex formation during mixing process and hence minimized the entrapment of gases.
- SiC particles as a reinforcement were introduced successfully into the Al alloy (Al-6082). Very fine particles of range 2-10 μm were uniformly dispersed the Al MMC, which is relatively difficult in conventional processes.

- Al alloys of composition Al-4.5wt% Cu was produced by the present continuous casting route, which has flexibility in the process and production. The structure of the alloy was confirmed through a detailed elemental analysis of the intra and inter grain regions.
- Grain refinement can be achieved with a homogeneous distribution of the GR in Al alloy system by processing through the said methodology.
- The illustrated continuous casting method is cost-effective than the other commercially available conventional processes with enhanced quality of cast product, showing less porosity, homogeneous distribution of the particles and alloying elements.

Acknowledgments

The authors acknowledge the Royal Academy of Engineering (UK & India, Industry-Academia Partnership Programme – 17-18, IAPP1R2/100109) for extending financial support. The authors would also like to express their gratitude to Bharat Al Company Limited, Korba, India for the supply of grain refiner rods.

Disclosure statement:

No potential conflict of interest was reported by the authors.

References

[1] Bandyopadhyay NR, Ghosh S, Basumallick A. New generation metal matrix composites. Mater Manuf Process 2007;22:679–82. https://doi.org/10.1080/104 26910701384872.

[2] Zhu L, Li N, Childs PRN. Light-weighting in aerospace component and system design. Propuls Power Res 2018;7:103–19. https://doi.org/10.1016/j.jppr.2018.04.001.

[3] Mandal A, Chakraborty M, Murty BS. Ageing behaviour of A356 alloy reinforced with in-situ formed TiB_2 particles. Mater Sci Eng A 2008;489:220–6. https://doi.org/10.1016/j.msea.2008.01.042.

[4] Mohanavel V, Rajan K, Arul S, Senthil P V. Production, Microstructure and Mechanical behavior of AA6351/TiB_2 composite synthesized by direct melt reaction method. Mater Today Proc 2017;4:3315–24. https://doi.org/10.1016/j.matpr.2017.02.218.

[5] Singla M, Singh L, Chawla V. Study of Wear Properties of Al-SiC Composites. J Miner Mater Charact Eng 2009;88:813–9. https://doi.org/doi:10.1111/j.1365-2745.2007.01245.x.

[6] Mahamani A, Jayasree A, Mounika K, Prasad KR, Sakthivelan N. Evaluation of mechanical properties of AA6061- TiB_2 / ZrB_2 in-situ metal matrix composites fabricated by K2TiF6 – KBF4 – K2ZrF6 reaction system 2015;10:185–200.

[7] Filatov YA, Yelagin VI, Zakharov V V. New Al-Mg-Sc alloys. Mater Sci Eng A 2000;280:97–101. https://doi.org/10.1016/S0921-5093(99)00673-5.

[8] Hashim J, Looney L, Hashmi MSJ. Metal matrix composites: production by the stir casting method. J Mater Process Technol 1999;92–93:1–7. https://doi.org/10.1016/S0924-0136(99)00118-1.

[9] Murty BS, Kori SA, Chakraborty M. Grain refinement of aluminium and its alloys by heterogeneous nucleation and alloying. Int Mater Rev 2002;47:3–29. https://doi.org/10.1179/095066001225001049.

[10] Hashim J. The Production of Cast Metal Matrix Composite by a Modified Stir Casting Method. J Teknol 2001;35:9–20. https://doi.org/10.11113/jt.v35.588.

[11] Rajan TPD, Pillai RM, Pai BC. Reinforcement coatings and interfaces in aluminium metal matrix composites. J Mater Sci 1998;33:3491–503. https://doi.org/10.1023/A:1004674822751.

[12] Panyam J, Chavanpatil MD. (12) Patent Application Publication (10) Pub . No .: US 2011 / 0020457 A1 Alginate core Patent Application Publication 2011;1.

[13] Kratochvíl J. Mechanism of grain refinement induced by severe plastic deformation. Mater Sci Forum 2011;667–669:617–22. https://doi.org/10.4028/ www.scientific.net/MSF.667-669.617.

[14] Tzamtzis S, Barekar NS, Hari Babu N, Patel J, Dhindaw BK, Fan Z. Processing of advanced Al/SiC particulate metal matrix composites under intensive shearing - A novel Rheo-process. Compos Part A Appl Sci Manuf 2009;40:144–51. https://doi.org/10.1016/j.compositesa.2008.10.017.

[15] Tran TT, Vo TT, Cho SC, Lee DH, Hwang WR. A stir casting system for drawdown of light particles in manufacturing of metal matrix composites. vol. 257. Elsevier B.V.; 2018. https://doi.org/10.1016/j.jmatprotec.2018.02.025.

[16] Zhu J, Jiang W, Li G, Guan F, Yu Y, Fan Z. Microstructure and mechanical properties of SiCnp/Al6082 aluminum matrix composites prepared by squeeze casting combined with stir casting. J Mater Process Technol 2020;283:116699. https://doi.org/10.1016/j.jmatprotec.2020.116699.

[17] Prasad NE, H. RJW. Aerospace Materials and Material Technology Vol. 1. vol. 1. 2016.

[18] Jiang W, Li G, Wu Y, Liu X, Fan Z. Effect of heat treatment on bonding strength of aluminum/steel bimetal produced by a compound casting. J Mater Process Technol 2018;258:239–50. https://doi.org/10.1016/j.jmatprotec.2018.04.006.

[19] Jiang Z, Fan Z, Jiang W, Li G, Wu Y, Guan F, et al. Interfacial microstructures and mechanical properties of Mg/Al bimetal produced by a novel liquid-liquid compound casting process. J Mater Process Technol 2018;261:149–58. https://doi.org/10.1016/j.jmatprotec.2018.06.013.

[20] Guan RG, Tie D. A review on grain refinement of aluminum alloys: Progresses, challenges and prospects. Acta Metall Sin (English Lett 2017;30:409–32. https://doi.org/10.1007/s40195-017-0565-8.

[21] Hashmi.J. The production of metal matrix composites using the stir casting By. J Mater Process Technol 1999;92–93:1–7.

[22] Bannaravuri PK, Birru AK. Strengthening of mechanical and tribological properties of Al-4.5%Cu matrix alloy with the addition of bamboo leaf ash. Results Phys 2018;10:360–73. https://doi.org/10.1016/j.rinp.2018.06.004.

[23] Kandpal BC, Kumar J, Singh H. Fabrication and characterisation of Al_2O_3/aluminium alloy 6061 composites fabricated by Stir casting. Mater Today Proc 2017;4:2783–92. https://doi.org/10.1016/j.matpr.2017.02.157.

[24] Ahmad SN, Hashim J, Ghazali MI. The effects of porosity on mechanical properties of cast discontinuous reinforced metal- matrix composite. J Compos Mater 2005;39:451–66. https://doi.org/10.1177/0021998305047096.

[25] Duverlie P, Castelain JM. Cost estimation during design step: Parametric method versus case based reasoning method. Int J Adv Manuf Technol 1999;15:895–906. https://doi.org/10.1007/s001700050147.

[26] Wang H, Zhou XH, Ruan XY. Research on injection mould intelligent cost estimation system and key technologies. Int J Adv Manuf Technol 2003;21:215–22. https://doi.org/10.1007/s001700300024.

[27] Feng SC, Zhang Y. Conceptual process planning - a definition and functional decomposition. Am Soc Mech Eng Manuf Eng Div MED 1999;10:97–106.

[28] Feng CX, Kusiak A, Huang CC. Cost evaluation in design with form features. CAD Comput Aided Des 1996;28:879–85. https://doi.org/10.1016/0010-4485(96)00009-7.

[29] Ou-Yang C, Lin TS. Developing an integrated framework for feature-based early manufacturing cost estimation. Int J Adv Manuf Technol 1997;13:618–29. https://doi.org/10.1007/BF01350820.

[30] Farineau T, Rabenasolo B, Castelain JM, Meyer Y, Duverlie P. Use of parametric models in an economic evaluation step during the design phase. Int J Adv Manuf Technol 2001;17:79–86. https://doi.org/10.1007/s001700170195.

[31] Society I. Parametric Estimating. 2008.

[32] Chougule RG, Ravi B. Casting cost estimation in an integrated product and process design environment. Int J Comput Integr Manuf 2006;19:676–88. https://doi.org/10.1080/09511920500324605.

Supporting Results

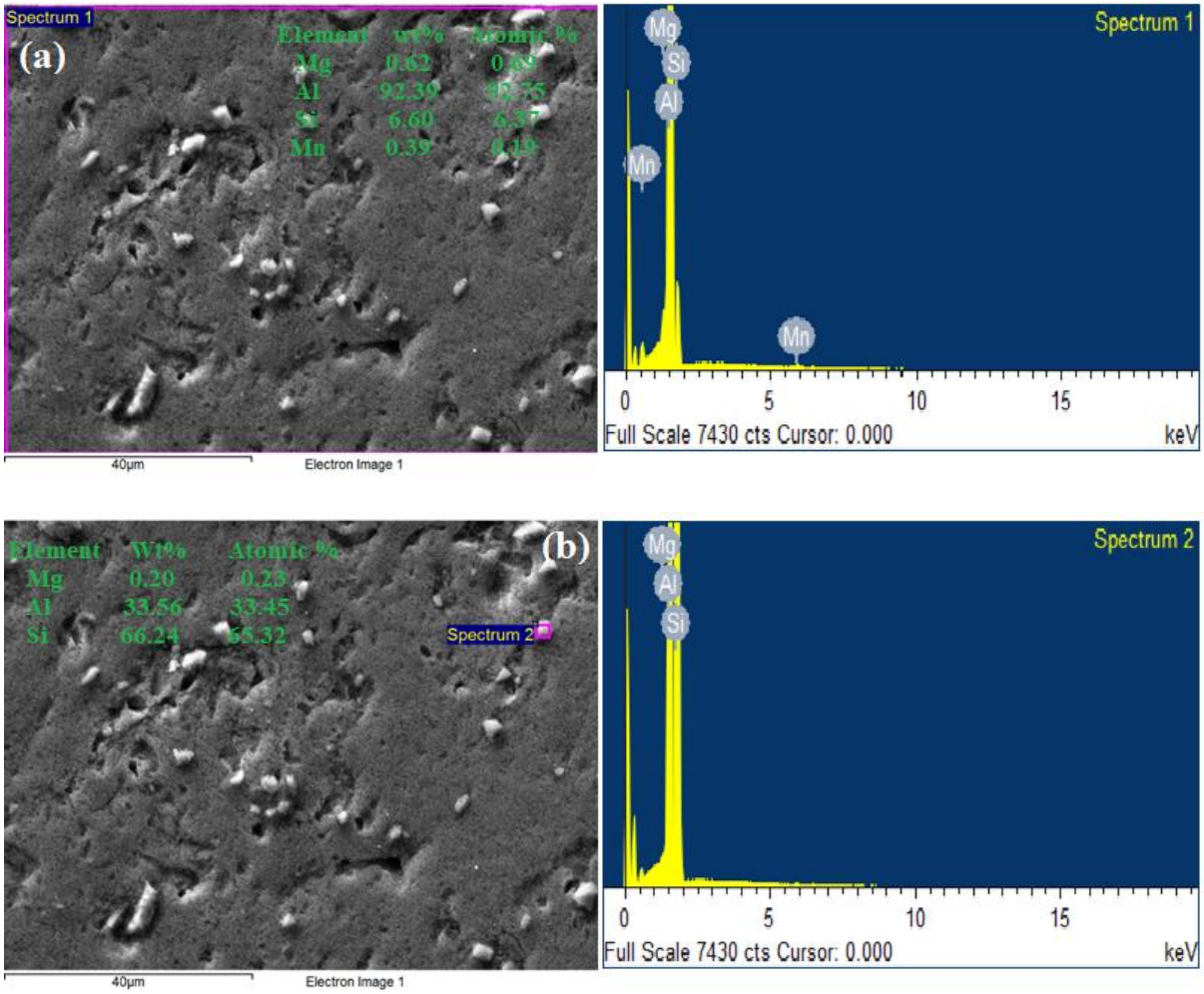

Fig S1: EDS of Al 6082-2wt% composite (a) Composite structure (b) embedded particle

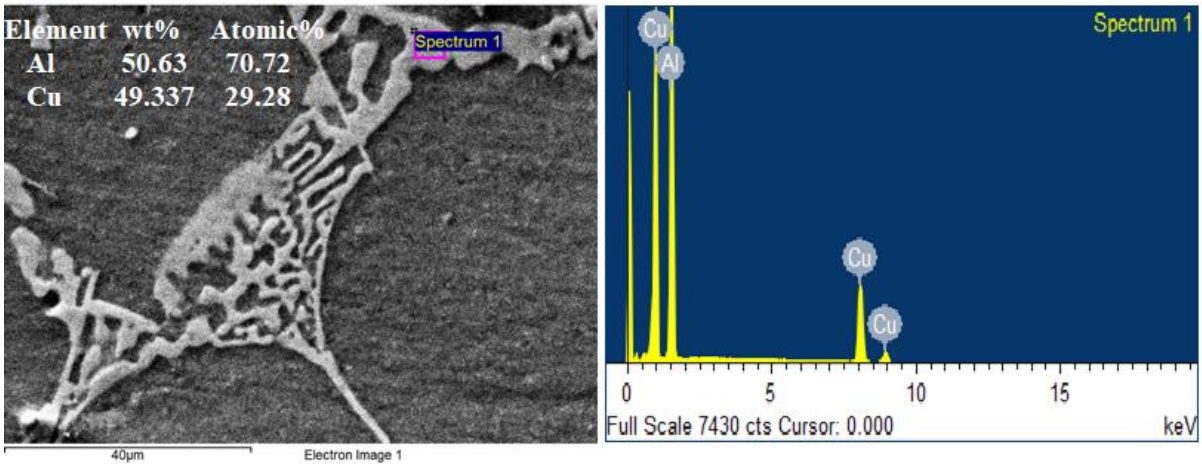

Fig S2: EDS of Al-4.5Cu binary alloy

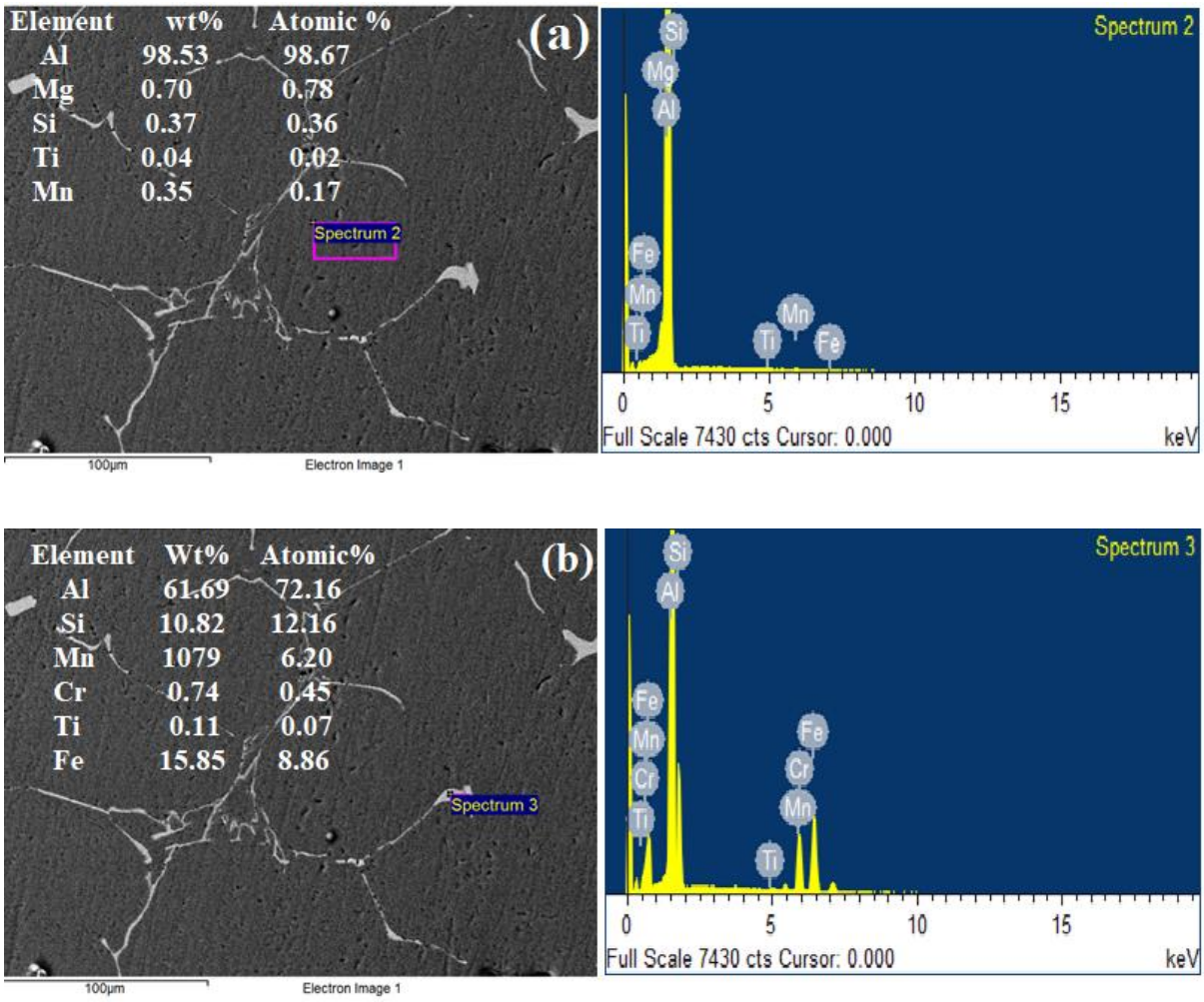

Fig S3: EDS of the grain refined structure (a) matrix (b) intermetallic

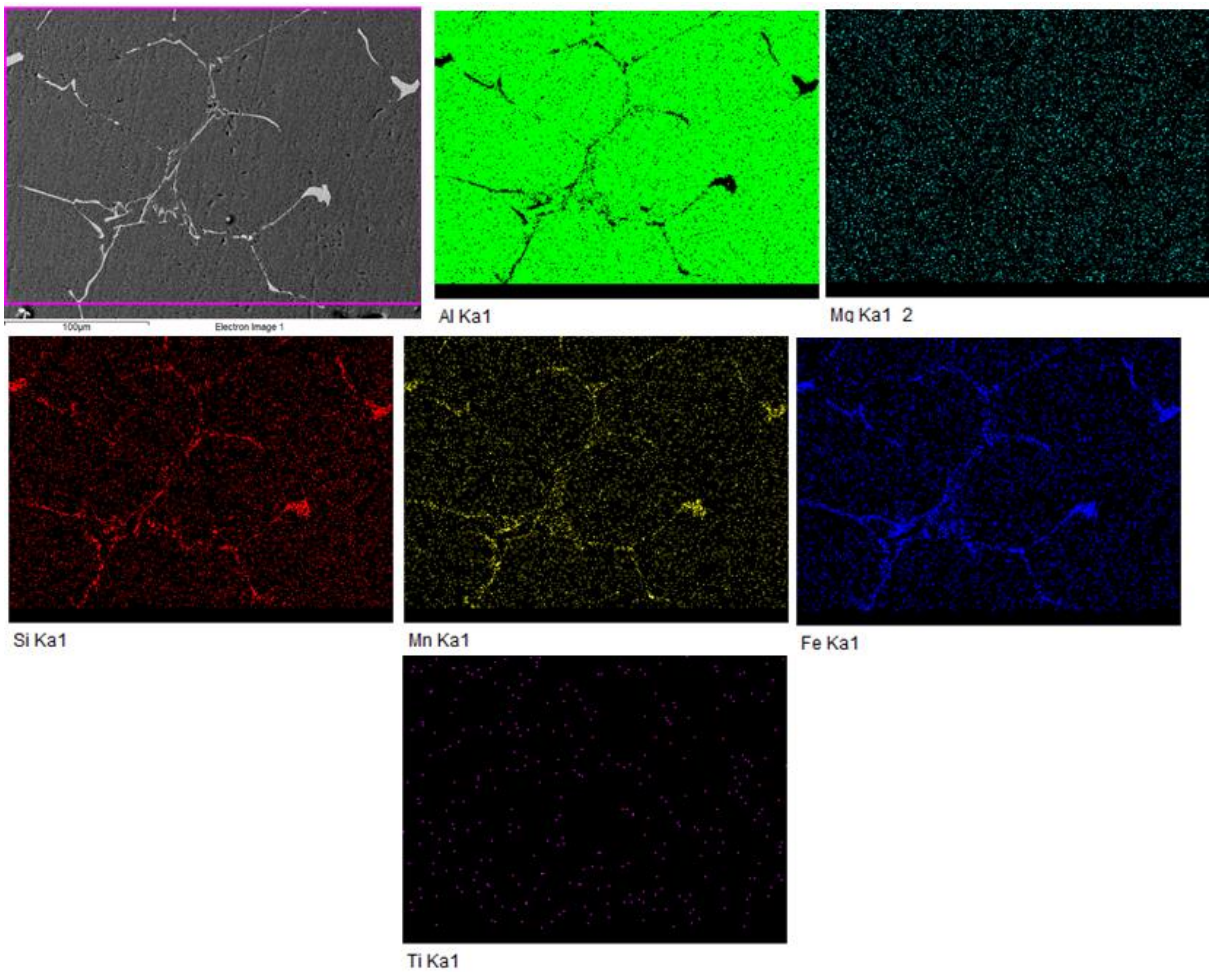

Fig S4: Mapping of Al 6082-2wt% Al5Ti1B grain refined alloy